Preparation and characterization of a novel bone graft composite containing bone ash and egg shell powder

GUNASEKARAN KRITHIGA and THOTAPALLI P SASTRY*

Central Leather Research Institute, Chennai 600 020, India

Abstract. Egg shells which were hitherto discarded as wastes were collected, purified and powdered into a particle size in the range of 5–50 μm. A composite bone graft material in cylindrical form was prepared using egg shell powder (ESP), bone ash (BA) and gelatin. These bone grafts were characterized for their FT–IR, TGA, XRD, SEM and mechanical properties. The mechanical studies indicate that the composite having a stoichiometric ratio of BA (3 g) and ESP (7 g) has shown better mechanical properties. X-ray diffraction (XRD) data indicated the crystallographic nature of BA is akin to hydroxyapatite (HA) and both BA and ESP did not lose their crystalline nature when bone grafts were prepared. This revealed that ESP may be used as a component in bone graft utilizing the solid waste from the poultry industry.

Keywords. Egg shell powder; bone ash; bone graft; gelatin; poultry industry; solid waste.

1. Introduction

Calcium and phosphorus are essential nutrients for all vertebrates and it is also well known that human bone contains ∼70% inorganic (apatite calcium phosphate) and 30% organic (mostly collagen) materials by weight. Hydroxyapatite, which resembles the inorganic part of bone, has received great attention in the world of biomaterials. Synthetic hydroxyapatite is prepared using a variety of chemical synthesis routes and reagents. Some of the techniques include wet processing (Monma and Kamiya 1987), dry processing (Fowler 1974), synthesizing via biological tissues (Liji Sobhana *et al* 2009; Sundaraseelan and Sastry 2007), sol–gel techniques (Yoshio *et al* 1990), electrochemical deposition etc. In our earlier studies, we have prepared calcined bone-based bone graft, and characterized and evaluated the same for its bone inducing capacity. We found that calcined bone exhibited similar crystallographic characteristics of hydroxyapatite (Noorjahan and Sastry 2005). In this study, we have used egg shell powder along with bone ash powder to prepare the implant and studied some of the physicochemical characteristics of the implant.

Egg shell which constitutes about 11% of the total weight of the whole egg contains about 91% of $CaCO_3$ (Rivera *et al* 1990; Nakano *et al* 2003). It is reported that 1,90,000 tonnes of egg shell is wasted in India and might be used as a calcium source in human nutrition (Schaafsma *et al* 2000). The biological behaviour of this natural material has also shown that it could be used as a bone substitute in the field of maxillofacial surgery (Dupoirieux *et al* 1995, 2000, 2001; Dupoirieux 1999). Egg shell particles ranging from 400–600 μm were bioassayed in the intramuscular pouches of rodents and their osteoinductive nature studied. It was reported that the particles did not exhibit osteoinductive capacities. After a 6-month study the authors have concluded that the egg shell powder could be used as a filler material in the bone defects of non-weight bearing areas. Sasikumar *et al* reported a simple combustion technique for synthesizing nanocrystalline hydroxyapatite powder from eggshell, diammonium hydrogen phosphate and citric acid. Using this method, the authors were able to control the particle size distribution and morphology of hydroxyapatite (Sasikumar and Vijayaraghavan 2006). Hydroxyapatite was also synthesized by several authors using egg shell as the starting material (Dasgupta *et al* 2004; Prabakaran *et al* 2005).

Hydroxyapatite is well known for its osteoconductive properties and widely used by clinicians worldwide (Shiny *et al* 2000; Gregory Lee *et al* 2005; Best *et al* 2008). In the present study, we have prepared bone grafts in cylindrical form using egg shell powder (ESP) and calcite bone powder along with gelatin, and partial characterization of these materials was carried out.

2. Experimental

2.1 *Methods*

2.1a *Preparation of bone ash*: Tibial bones of the cattle were collected from a nearby slaughter house. The bones

---

*Author for correspondence (sastrytp@hotmail.com)

were cut into $2 \times 2''$ pieces using a prebeaker. Then the bone pieces were incinerated at 300°C and ashed at 750°C for about 5 h. This treatment made organic matter present in the bone to get volatilized and resulted in the formation of bone ash, which was nothing but the inorganic part of the bone which was denoted as bone ash (BA).

2.1b *Preparation of gelatin*:

Gelatin powder from bovine source having 250 Bloom strength was kindly supplied by Maruthi Gel Company Ltd, Trichy, India. Five g of gelatin powder was dissolved in 12 ml of water at 50°C with constant stirring. This solution was denoted as 'G'.

2.1c *Preparation of egg shell powder (ESP)*:

Egg shells were collected from a nearby restaurant and washed thoroughly, initially in tap water and later in distilled water. The adhering membrane was separated manually and shells were dried at room temperature (30°C). Later the shells were crushed using a domestic mixer, to a particle size in the range of 5–50 μm. The powdered ESP was stored in polythene covers at room temperature (30°C) till further use.

2.1d *Preparation of ESP with G (ESP–G)*:

To 6 ml of gelatin solution, 10 g of ESP was added, contents were mixed well and made into paste using a mortar and pestle. With the help of glass tube with a diameter of 1·2 cm the paste was extruded as cylindrical implant. After 2 h of air drying the implants were cured at 80°C for 12 h.

2.1e *Preparation of BA with G (BA–G)*:

To 6 ml of gelatin solution 10 g of BA was added, contents were mixed well and made into paste using a mortar and pestle. The implant preparation was followed as explained in the case of ESP–G.

2.1f *Preparation of ESP–BA with G (ESP–BA–G)*:

To a mixture containing different amounts of ESP and BA (table 1), 6 ml of gelatin solution was added, and contents were mixed well and made into paste using a mortar and pestle. The implant preparation was followed as explained in the case of ESP–G.

2.2 *Characterization*

2.2a *Compressive strength*:

Cylindrical specimens (diameter 1 cm, height 0·8 cm) were prepared and allowed to set at 30°C for 24 h and then cured at 80°C. To measure the compressive strength, samples were loaded along the cylindrical axis in between the platens of the machine at a crosshead speed of 1 mm/min, using Instron 4501 model. The compre-

Table 1. Mechanical properties of ESP, BA and ESP–BA–G composite.

Sl. no.	Sample	Compressive strength (MPa)	Tensile strength (MPa)
1.	ESP-G	8·24	37
2.	BA-G	3·31	30
3.	BA+ESP(7:3 g)	4·1	32
4.	BA+ESP(5:5 g)	4·3	34
5.	BA+ESP(3:7 g)	4·7	35

The results given are an average of three specimens.

ssive strength was calculated from the break load and dimensions of the pellets. The results given are an average of three specimens (table 1).

2.2b *Tensile strength*:

Cylindrical specimens (diameter, 0·5 cm, height 0·8 cm) were prepared and allowed to set at 37°C for 24 h and cured at 80°C. Tensile strength of the sample was measured using Universal Testing Machine (INSTRON model 1405). The results given are an average of three specimens (table 1).

2.2c *Infrared spectroscopy (FT–IR)*:

The IR spectra of the samples prepared were recorded in the 4000–400 cm^{-1} range using Nicolet Impact 400 Fourier Transform Infrared spectrophotometer with KBr pellet containing 2–6 mg of the sample.

2.2d *X-ray diffractometry (XRD)*:

The samples were analysed on a Siemens 500 X-ray powder diffractometer in a flat plane geometry using a source of Cu Kα of wavelength, 1·5406 Å. The patterns were recorded in the region of 10–90° ($2\,\theta$) in steps of 0·001° with a counting time of 1 s in each step.

2.2e *Thermogravimetric analysis*:

TGA of the samples prepared were carried out using a Seiko SSC 5200 H in nitrogen atmosphere (80 ml/min) at a heating rate of 10°C/min. Primary weight loss of these materials as a function of temperature was recorded using this study.

2.2f *Scanning electron microscopy (SEM)*:

Dried samples were coated with gold ions using an ion coater (fisons sputter coater) under the following conditions: 0·1 Torr pressure, 200 mA current and 70 s coating time. Surface structure was visualized by scanning electron microscope (SEM model: LEICA stereoscan 440) using a 15 kV accelerating voltage.
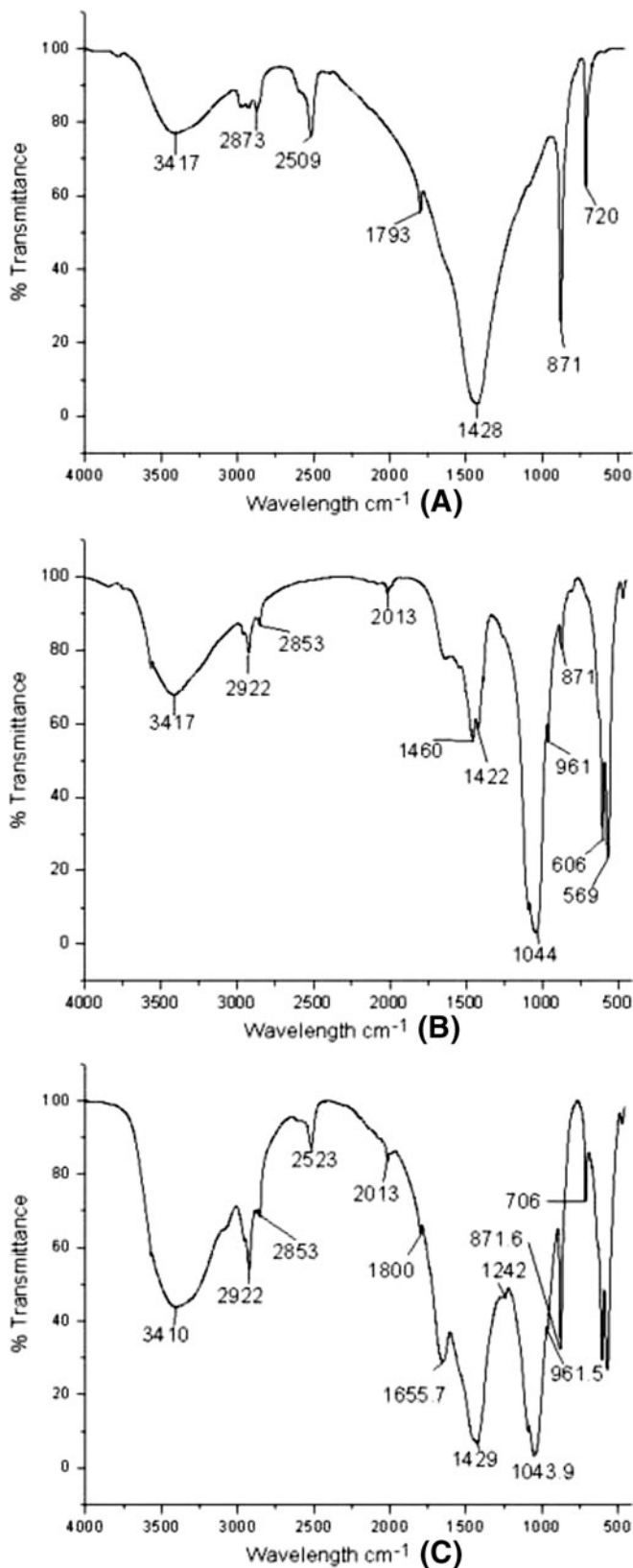
Figure 1. FTIR spectra of (**A**) ESP, (**B**) BA and (**C**) ESP+BA+G.

3. Results and discussion

3.1 *FTIR*

FTIR spectra of ESP, BA and BA–ESP–G are shown in figures 1A, B and C, respectively. The FTIR spectrum of ESP shows the absorption bands of carbonate at 871 cm^{-1} and a broad peak at around 1428 cm^{-1}. This data confirms the presence of CaCO$_3$ in the egg shell powder. In the case of BA (figure 1B), FTIR spectrum shows peaks at 961∼1044 cm^{-1} and 569∼606 cm^{-1} representing the characteristic well crystallized apatite phase. The peak at 961 cm^{-1} corresponds to ν_1 stretching mode and 1044 cm^{-1} represents ν_3 vibration mode of phosphate groups. The sharp peaks at 569∼606 cm^{-1} are assigned to the bending mode of phosphate. The absorption bands at 1422–1460 and 876 cm^{-1} are due to the vibration mode of carbonate groups. IR spectrum of BA is similar to that of HA which was also confirmed in our earlier studies (Noorjahan and Sastry 2005). In the FTIR spectrum of BA–ESP–G (figure 1C), we can find the peak characteristic of both BA and ESP along with amide absorption bands at 1657 (amide I), and 1242 (amide III) representing gelatin.

3.2 *XRD*

Figures 2A–C represent the XRD patterns of ESP, BA and BA–ESP–G. A good agreement between the experimental data for BA and JCPDS standard for calcium hydroxyapatite (ref. code:89-6439) both in terms of intensity and despairing was obtained. The strong diffraction peaks corresponding to hydroxyapatite at 2 θ position, 31·6 (211) plane together with other two peaks, 32·04 and 32·7, confirmed the structure of hydroxyapatite in crystal form (Ahmed and Ahsan 2008). In the case of ESP a strong peak at 29·3 for CaCO$_3$ was observed. Other peaks are of less intensity and insignificant and this is in agreement with XRD of earlier studies (Park *et al* 2007). In the case of BA and ESP composite, the characteristic peaks of HA and ESP is seen. This data indicates that BA contains the crystallographic structure of hydroxyapatite and when it is mixed with gelatin and ESP the crystallinity of the composite is not lost.

3.3 *Mechanical strength*

Among the mechanical properties of bone repair materials, compressive strength is the most widely explored one. The strength of the composites depends on various factors like particle size of individual components, nature of adhesives and percentage of moisture present in the sample. The variation in the compression strengths of various compositions of BA–ESP–G are given in table 1. ESP–G alone has shown better compressive strength compared to other samples. The
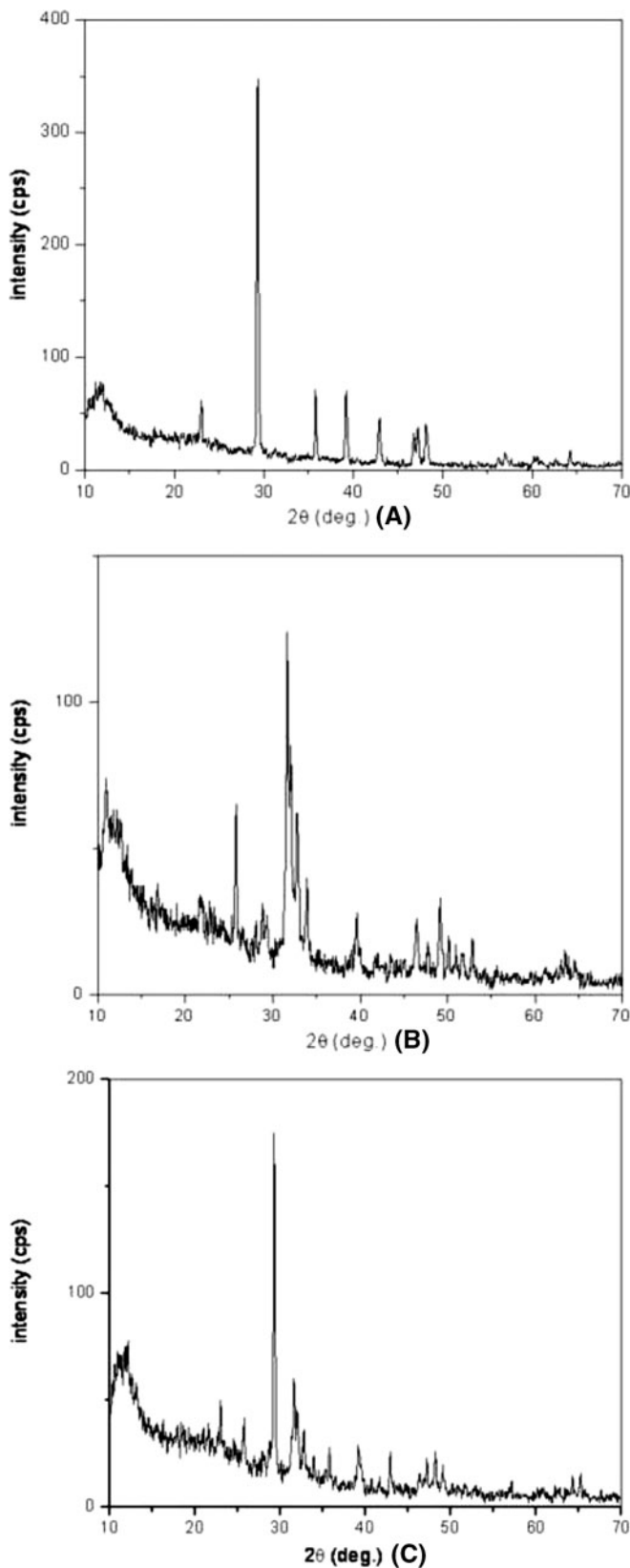
composite having stoichiometric ratio BA (3) and ESP (7) has shown better compressive strength (4·7 MPa) among the composites prepared. This compressive strength is less compared to those of synthetic HA implant (13–20 MPa) and natural bone (165 MPa). These implants cannot be used in defects of weight bearing bones, however, they may be used in the defects of non-weight bearing bones, e.g. maxillofacial bones, spinal cord bones etc.

3.4 *Tensile strength*

The tensile strength of ESP–G was found to be much higher than the BA–G (table 1). The composite having stoichiometric ratio of BA (3)–ESP (7)–G gave better tensile strength (35 MPa) compared with other composites prepared.

3.5 *Thermogravimetric analysis*

The thermogram of ESP–BA–G composite is shown in figure 3. A three-step weight loss was observed. About 4% weight loss was observed up to 260°C due to loss of water or bound water. The second weight loss of 13% was observed between 260°C and 616°C which may be attributed to the decomposition of protein (gelatin, which is the binder) into CO_2 and H_2O. The third weight loss of 20% which occurred between 616°C and 735°C may be attributed to the decomposition of $CaCO_3$ component in ESP into CaO and CO_2. About 63·5% of inorganic material is supposed to be hydroxyapatite, but CaO still remains above 735°C.

3.6 *Scanning electron microscope*

The surface morphology of BA–ESP–G composite is shown in figure 4. The porous nature of the composite is seen in lower magnification (300×) as well as in higher magnification. SEM pictures indicate irregular pores ranging from 50–150 μm which is favourable for the bone ingrowth (Zang
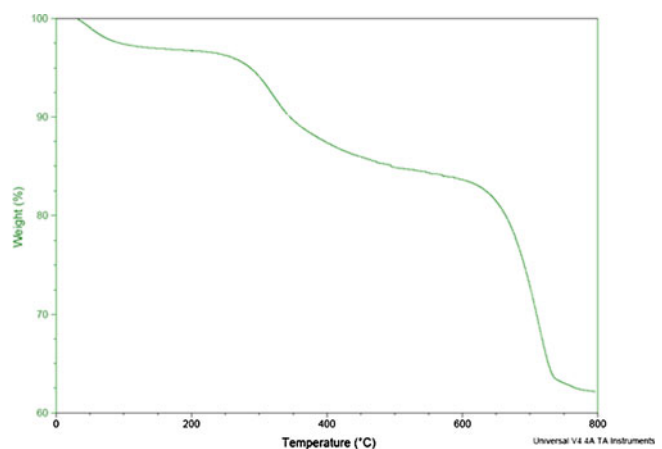
Figure 2. X-ray diffraction patterns of (**A**) ESP, (**B**) BA and (**C**) ESP+BA+G.

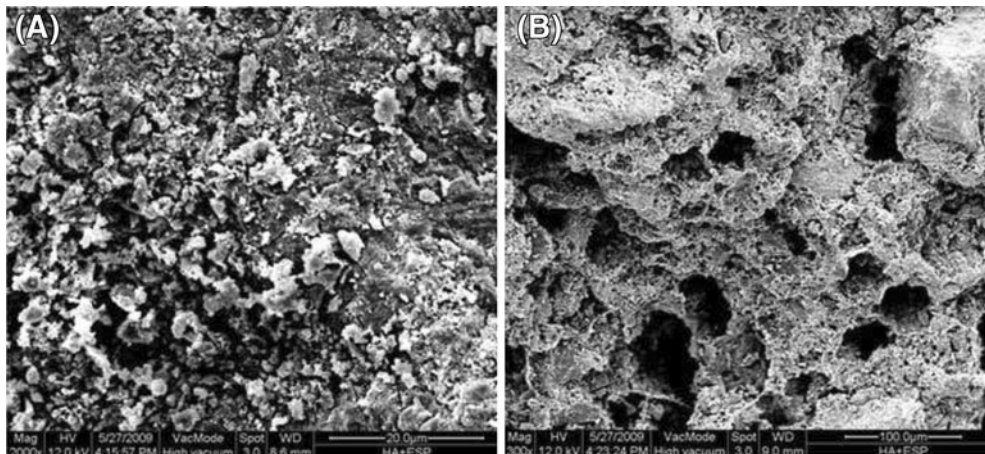**Figure 3.** Thermogravimetric analysis graph of ESP+BA+G.

Figure 4. Typical SEM images of ESP+BA+G at (**A**) 2000× and (**B**) 300×.

et al 2003). There is no distinct difference for the pore size distribution in the implant.

The FTIR spectrum of ESP has exhibited absorption peaks comparable to those of $CaCO_3$, similar results were observed in the case of XRD studies also. Previous studies (Balliga *et al* 1998; Park *et al* 2007) have shown that the hen egg shell powder is a safe bone substitute which is easily available. FTIR spectrum and XRD of BA exhibited absorption peaks comparable to those of hydroxyapatite (Noorjahan and Sastry 2005). In earlier studies, calcined bone gave clinically good results when the same was used in rabbit mandible defects (Wafaa *et al* 1994). Based on these studies, we have prepared the ESP–BA–G composite. The compressive strength of the composite was found to be less, hence it may be used in defects of non-weight bearing bones such as maxillofacial and spinal cord bones. This will not only reduce the cost of bone graft but also egg shell waste can be utilized for this purpose.

4. Conclusions

The present study explored the possibility of using ESP along with BA as a bone graft material. Further studies may confirm the possibility of converting this solid waste of poultry industry into wealth.

References

Ahmed Samina and Ahsan Mainul 2008 *Bangladesh J. Sci. Ind. Res.* **43** 501

Balliga M, Davies P and Dupoirieux L 1998 *Rev. Stomatol. chir Maxillofac.* **99** 86

Best S M, Porter A E, Thian E S and Huang J 2008 *J. Eur. Ceram. Soc.* **28** 1319

Dasgupta P, Singh A, Adak S and Purohit K M 2004 *International symposium of research students on materials science and engineering, Chennai, 1*

Dupoirieux L 1999 *J. Oral Maxillofac. Surg.* **37** 467

Dupoirieux L, Pourquier D and Souyris F 1995 *J. Craniomaxillofac. Surg.* **23** 187

Dupoirieux L, Neves M and Pourquier D 2000 *J. Oral Maxillofac. Surg.* **58** 40

Dupoirieux L, Pourquier D, Neves M and Teot L 2001 *J. Craniofac. Surg.* **12** 53

Fowler B O 1974 *Inorg. Chem.* **13** 207

Gregory Lee Y, Ajay S, Darryl D'Lima D, Pamela Pulido A and Clifford Colwell W 2005 *J. Arthroplasty* **20** 57

Liji Sobhana S S, Sundaraseelan J, Sekar S, Sastry T P and Mandal A B 2009 *J. Nanopart. Res.* **11** 333

Monma H and Kamiya V 1987 *J. Mater. Sci.* **22** 4247

Nakano T, Ikawa N I and Ozimek L 2003 *Poult. Sci.* **82** 510

Noorjahan S E and Sastry T P 2005 *J. Biomed. Mater. Res.* **B75** 343

Park Jin-Woo, Bae Sang-Ryul, Suh Jo-Young, Lee Dong-Hee, Kim Sang-Hyun, Kim Hyungiun and Lee Chong-Soo 2007 *J. Biomed. Mater. Res.* **87** 203

Prabakaran K, Balamurugan A and Rajeshwari S 2005 *Bull. Mater. Sci.* **28** 115

Rivera E M, Araiza M, Brostow W, Castano V M, Diaz-Estrada J R and Rogelio Rodriguez 1990 *J. Mater. Lett.* **41** 128

Sasikumar S and Vijayaraghavan R 2006 *Trends Biomater. Artif. Organs* **19** 70

Schaafsma A, Pakan I, Hofstede G J H, Muskiet F A J, Van Der Veer E and De Vries P J F 2000 *Poultry Sci.* **79** 1833

Shiny V, Ramesh P, Sunny M C and Varma H K 2000 *Mater. Lett.* **46** 142

Sundaraseelan J and Sastry T P 2007 *J. Biomed. Nanotech.* **3** 401

Wafaa I A F, Osiris W G, Shamael S M and Khalil M R 1994 *Biomaterials* **20** 475

Yoshio M, Kazuo M and Sumio S 1990 *J. Ceram. Soc. Jap.* **98** 1255

Zang S M, Cui F Z, Liao S S, Zhu Y and Han L 2003 *J. Mater. Sci.* **14** 641